

*Invited paper***Few-cycle-driven XUV laser harmonics: generation and focusing****M. Schnürer¹, Z. Cheng¹, M. Hentschel¹, F. Krausz¹, T. Wilhein^{2,*}, D. Hambach², G. Schmahl², M. Drescher³, Y. Lim³, U. Heinzmann³**¹Institut für Photonik, Technische Universität Wien, Gusshausstr. 27-29, 1040 Wien, Austria

(Fax: +43-1/58801-38799, E-mail: schnuerer@tuwien.ac.at)

²Institut für Röntgenphysik, Universität Göttingen, Geiststr. 11, 37073 Göttingen, Germany³Lehrstuhl für Molekül und Oberflächenphysik, Universität Bielefeld, Universitätsstr. 25, 33615 Bielefeld, Germany

Received: 1 October 1999/Revised version: 10 February 2000/Published online: 24 May 2000 – © Springer-Verlag 2000

Abstract. We have investigated the use of sub-10-fs near-infrared laser pulses to generate high-order harmonic radiation efficiently in the wavelength region between 30 to 10 nm. The ultrashort rise time of the driver pulses allows harmonics to be produced at low ionization levels and hence to grow coherently over propagation lengths becoming comparable to the XUV absorption lengths in the noble gas medium. As a result, absorption-limited harmonic generation has been extended to the 10-nm range for the first time. Harmonic conversion efficiencies of $(3\text{--}4)\times 10^{-8}$ in the range of 10–13 nm in neon and some two orders of magnitude higher at around 30 nm in argon have been obtained in simple gas tube targets under these conditions. Preliminary focusing tests with 13-nm harmonic radiation have been carried out with a specially designed zoneplate and a spherical Mo/Si multilayer mirror and have resulted in spot sizes of about 2 microns. Our experiments aim at paving the way to nonlinear optics in the soft-X-ray regime.

PACS: 42.65.Ky; 41.50.+h; 42.50.Hz; 42.65.Re

Spectroscopic investigations in the XUV and soft-X-ray wavelength region on a time scale of nuclear motion or electronic transitions are of interest for gaining insight into the dynamics of chemical reactions, phase transitions, or inner-shell electronic relaxation. The generation of intense femtosecond XUV/X-ray pulses constitutes an enabling technology for extending time-resolved spectroscopy into the short-wavelength regime. To this end, the development of ultrafast-laser-driven XUV/X-ray sources is being pursued in a number of high-intensity laser laboratories. Here we study high-order harmonic radiation produced with intense short laser pulses which constitutes a promising source of coherent ultrashort XUV/X-ray pulses [1–4]. Its practical use critically depends on the photon flux achievable. Hence the conversion efficiency of laser to high harmonic energy is

a key parameter for these sources. We demonstrate that sub-10-fs laser pulses allow the coherence length of harmonic radiation to be extended to several times the XUV absorption length in the interaction gas volume down to wavelengths as short as 10 nm and present first focusing experiments in this wavelength range.

1 Experimental setup

The XUV/soft-X-ray harmonic radiation is generated by focusing linearly-polarized 7-fs laser pulses carried at a wavelength of ≈ 790 nm into an argon and neon quasi-static gas cell formed by a nickel tube [4] placed at focus position. The effective interaction lengths have been varied between 0.3 mm and 8 mm in the experiments. The few-cycle pulses are produced by a Ti:sapphire-based laser system supplemented with a hollow-fiber-chirped-mirror post-compression system [5]. Pulse energies of 0.7 mJ are delivered at a 1-kHz repetition rate in a diffraction-limited beam. In the experiments the laser beam has been focused to a $1/e^2$ diameter of $2w_0 \approx 60$ μm (0.7 mm confocal parameter, $f = 200$ mm spherical mirror) or, alternatively, ≈ 120 μm (2.8 mm confocal parameter, $f = 400$ mm spherical mirror), resulting in effective temporal peak intensities (averaged over $A_{\text{eff}} = \pi w_0^2$) up to $I_{\text{peak}} = 5 \times 10^{14}$ W/cm² and 2×10^{15} W/cm², respectively. The spectral characterization of the harmonic radiation is performed by a grazing incidence spectrograph. Absolute photon yields are measured with an unbiased silicon XUV-photodiode (X-UV50C, UDT Sensors, calibration data provided by the manufacturer) and an electrometer. In order to block the laser light completely, three Al filters (200-nm Al embedded in $\approx 2 \times 30$ -nm Al₂O₃ layers) had to be placed in front of the photodiode. The calculated filter transmittivity in the relevant wavelength range has been verified with our harmonic source and the spectrograph.

Both diffractive and multilayer X-ray optics have been employed for focusing the generated harmonic radiation near 13 nm. A specially-designed Si-Ge zone plate with a diameter of 0.6 mm and a focal length of 10 mm has been manufac-

*Current address: Engineering Physics, RheinAhr Campus Remagen, Süddallee 2, 53424 Remagen, Germany

tured at the University of Göttingen [6]. When uniformly illuminated with 13-nm coherent radiation, a diffraction-limited focused beam diameter of ≈ 300 nm is predicted to be achievable in its focal plane. Approximately 5% of the incident XUV power is diffracted into the focused first order. A spherical Mo/Si multilayer mirror consisting of 28 periods has also been prepared for focusing the harmonic beam. The multilayer stack has been designed and deposited on a super-polished substrate by means of e-beam evaporation in UHV with in situ thickness and roughness control [7], resulting in reduced interface roughness [8], at the University of Bielefeld. The mirror has a focal length of 35 mm, an aperture of 10 mm, and is operated at an angle of incidence of 3.5° . Its reflectivity at about 13 nm is expected to be slightly smaller than the value of 64% measured for a similar mirror with 50 periods. Ray-tracing calculations predict the feasibility of a (non-diffraction-limited) focal diameter of ≈ 1 μm .

2 XUV harmonic emission in the absorption limit

Using the target and laser focusing geometries described above we have studied XUV harmonic emission from argon and neon gas media. For comparison, we also present some data about soft-X-ray harmonic emission down to wavelengths less than 3 nm from helium driven with 5–7-fs pulses at $4\text{--}5 \times 10^{15}$ W/cm² peak intensity levels. Part of the results presented below were recently reported in [9, 10].

Optimum XUV harmonic yields from both argon and neon have been obtained at pressures ranging from 0.3 to 0.4 bar, respectively. In argon, the pressure-optimized signal was found to vary within only a factor of 2–3 for the different target geometries and the distribution of the harmonic spectrum did not show significant variations. Highest signals have been obtained with comparably high laser driving intensities of 2×10^{15} W/cm². The observed harmonic spectrum peaks around the 25th–29th harmonics (32–27 nm), close to the absorption minimum of argon, suggesting that XUV-absorption significantly affects harmonic production under our experimental conditions. The refraction indices of the relevant rare gas for the laser light and for the XUV-light were taken from [11] and [12], respectively. The absorption length for the 25th harmonic is about 165 μm which is only 35% of the estimated geometrical coherence length of 470 μm , which is extended by the net positive refractive index of the argon gas at low ionization levels [13] present around the instant when these harmonics first appear on the leading edge of the sub-10-fs driver pulse.

Experimental data are compared with results obtained from numerical simulations. In our model, the atomic dipole acceleration is calculated using the quantum theory of Lewenstein et al. [14] combined with the ADK ionization rate [15]. Propagation of the laser (which includes the evolution of the laser intensity) and XUV pulse in the ionizing gas is computed by numerically solving Maxwell's equations in one spatial dimension. In the following discussion we consider the geometrical, plasma, and neutral phase advance whereas the dipole phase [17] under our conditions evolves notably on a scale of several mm and hence can be neglected.

The limiting role of absorption in the generation of XUV harmonics at around 30 nm under our experimental conditions is confirmed by Fig. 1. Here, the pressure dependence

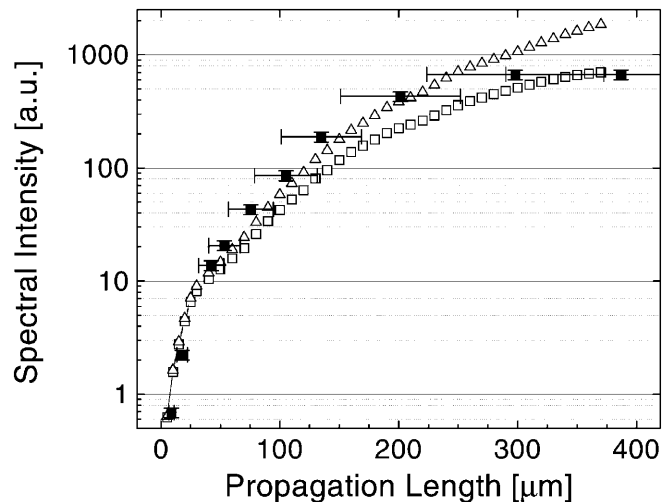


Fig. 1. Calculated (*open squares*) and measured (*full squares*) evolution of the 27th harmonic upon propagation through the argon target at a pressure of 0.7 bar for $\tau_p = 7$ fs, $2w_0 = 60$ μm , and $I_p = 5 \times 10^{14}$ W/cm². The error bars result from uncertainties in estimating the effective propagation length L_{eff} and assessing the pressure in the interaction region. The *triangles* depict the calculated harmonic signal in the absence of XUV absorption

of the harmonic yield from a thin target (interaction length shorter than geometric coherence length) is mapped into a dependence on the propagation length at a fixed pressure and compared with the computed growth of the harmonic signal in the interaction region. With the XUV absorption absent the signal continues to grow at a considerable rate up to the boundary of the simulation interval, providing conclusive evidence for the limiting role of XUV absorption in the harmonic generation process.

In neon we obtained best harmonic emission performance with interaction lengths of 2–3 mm at a pressure of approximately 0.4 bar. Calculations suggest that under *few-cycle* excitation the ionization level is low ($\approx 0.5\%$) enough for the positive contribution of neutral atoms to the refractive index to overcompensate the negative plasma contribution and Gouy shift even at wavelengths as short as 10–15 nm. As a result, we may expect a similar gas-pressure-dependent phase-matching effect as observed at much longer wavelengths (≈ 30 nm in argon) by Rundquist et al. [13] (as well as in our experiments described above) to occur for the first time at the border of the soft-X-ray wavelength range around 10–13 nm.

This expectation is verified by measuring the yield of the 61st few-cycle-driven laser harmonic from two different neon targets as a function of pressure. The results of these measurements are shown in Fig. 2. The harmonic signal saturates at a much lower value of the product of gas density and interaction length in the thin ($L_{\text{eff}} \approx 0.3$ mm) target as compared to the corresponding value in the thick target ($L_{\text{eff}} \approx 3$ mm), resulting in almost an order of magnitude higher yield in the latter configuration. This means that a significantly (\approx factor of 4) higher number of atoms contribute coherently to the emitted harmonic signal in the thicker target than is the case in the thinner one, indicating correspondingly improved phase-matching conditions. As a matter of fact, the pressure yielding the maximum signal is found to be close to the estimated value [10] needed for mutual compensation of the geometrical, plasma, and neutral atom phase advance under

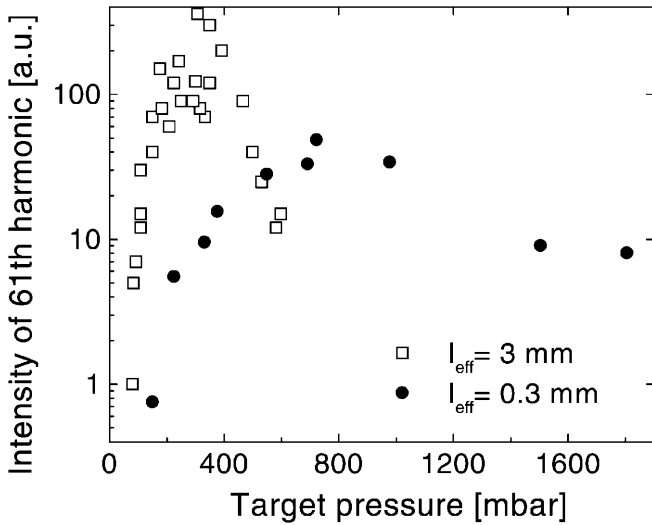


Fig. 2. Intensity of the 61st laser harmonic @ 13 nm as a function of neon gas pressure obtained with $\tau_p = 7$ fs, $2w_0 = 60$ μm , and $I_p = 5 \times 10^{14}$ W/cm² from two targets with different interaction lengths L_{eff}

our conditions. The sensitivity of this compensation clearly manifests itself in (i) the pronounced signal peak and (ii) the enhanced signal fluctuation due to possible small pressure variations and the stronger influence of laser intensity fluctuations at the phase matching point.

The pressure balancing is possible because the ionization level for $I_p = 5 \times 10^{14}$ W/cm² (laser peak intensity) reaches only $\approx 0.5\%$ during the production of harmonics in the range of 10–15 nm, resulting in a net positive material contribution to the refractive index of vacuum at the laser wavelength. This pressure-dependent contribution compensates the geometric phase advance (Gouy phase shift) at a pressure of 0.3–0.4 bar. This moderate pressure calls for an extended interaction length allowing us to increase the number of coherently-driven emitters until absorption come into play. If the interaction length at the phase-matching pressure considerably exceeds the XUV absorption length the coherent signal growth is stopped. At 0.4 bar in Ne the absorption length of the 61st harmonic is about 230 μm , hence according to Constant et al. [16] full saturation can be expected for interaction lengths of 2–3 mm.

Again, for assessing the role of XUV absorption, the measured pressure dependence of the harmonic yield from the thin (0.3 mm) target can be mapped into a dependence on the propagation length at a fixed pressure (0.4 bar) and compared with the computed growth of the harmonic signal in the interaction region (Fig. 3). This mapping is legitimized by the geometric dephasing length (about 0.7 mm for harmonic order H61) and the atomic dipole dephasing length being larger than the interaction region and therefore related dephasing effects are negligible. All other effects (absorption, free-electron dephasing, etc.) scale with $n \times L$ (density \times propagation length), allowing us to map density dependence into propagation length dependence and vice versa. Yet a comparison of the measured data with the results of computer simulations for absorption being present and absent reveals that absorption significantly affects the harmonics output even from the thin target, implying that the absorption

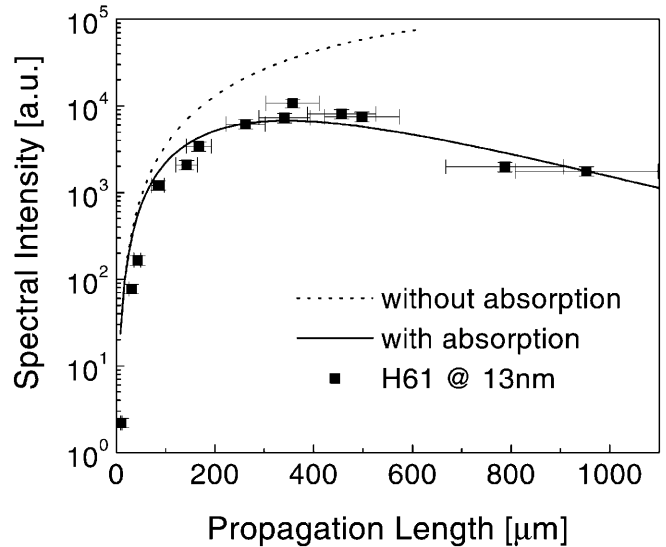


Fig. 3. Evolution of the 61st harmonic (*squares* – measured, *lines* – computed) upon propagation in the neon target at a fixed pressure of 0.4 bar. The errors bars depict systematic errors resulting from an uncertainty in estimating the effective interaction length, see text for further details

limit is fully exploited with the thick target. The observed signal decrease for long propagation lengths can be assigned to a decrease in peak laser intensity as a consequence of self-phase-modulation-assisted dispersive pulse broadening in the simulation.

3 Few-cycle-driven laser harmonic yields from 35 nm to 2.5 nm

The high harmonic production efficiencies have been derived from the photocurrents induced in a silicon XUV photodiode placed behind a series of aluminum filters. The spectral transmittivity of the Al filter used and the spectral intensity distribution of the harmonics were measured with the spectrograph. Data below the Al L-edge (17 nm) have been obtained from spectral measurements assuming a flat grating-detector response. The harmonic conversion efficiency evaluated from these measurements along with the results of computer simulations under our experimental conditions are plotted in Fig. 4. The numerically simulated curves for harmonic generation in Ar, Ne, and He have been fitted to the measured data using only a single multiplicative constant to the XUV intensity as a fit parameter. In the case of He, the ionization rate has been numerically calculated from the Schrödinger's equation [18]. The efficiency data below 10 nm wavelength from He gas targets (0.3 mm thick tubes at typically 4–5 bar pressure) have been obtained by comparing the levels of signals from Ne and He acquired with the same grating spectrometer – Channeltron detector – lock-in amplifier – system. Because of a possibly increasing error for extrapolations far from the Al L-edge we regard the presented efficiencies down to the water window (4.4–2.3 nm) as order-of-magnitude estimates. Nevertheless, the measured decrease of the signals is quite well reproduced qualitatively by the simulation [19].

Efficiencies of 10^{-7} to 10^{-5} in the range of 25–50 nm have also been measured in other recent experiments [13, 16, 20, 21] where different target setups (gas-filled hollow-core

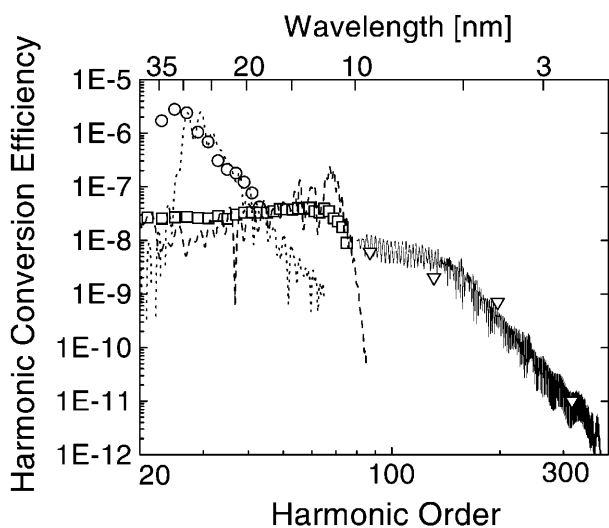


Fig. 4. Harmonic production efficiency in argon, $L_{\text{eff}} = 3$ mm, $p = 0.3$ bar (circles), in neon, $L_{\text{eff}} = 3$ mm, $p = 0.4$ bar (squares) at $I_p = 2 \times 10^{15}$ W/cm² and $I_p = 5 \times 10^{14}$ W/cm² and in He (triangles) with $L_{\text{eff}} = 0.3$ mm, $p \approx 4$ bar at $I_p = 4 \times 10^{15}$ W/cm², respectively, using 7-fs Ti:sapphire laser pulses and calculated spectra: dotted, dashed and full lines, respectively

fibers or gas jets) have been used [22]. Comparative measurements of these two sources in the context of the limiting role of absorption have recently been done at wavelengths around 60 to 35 nm by Constant et al. [16]. These experiments as well as a comparison of our data with those obtained by Rundquist et al. [13] at around 30 nm indicate that with similar driver pulses comparable efficiencies within one order of magnitude can be obtained with waveguide and gas jet or tube targets. Realizing absorption-limited high-harmonic generation in the wavelength range down to 10 nm implies that further improvements by several orders of magnitude should not be expected. Requirements on criteria such as source stability, alignment sensitivity, and gas consumption will determine which target geometry is to be chosen for specific applications.

4 Focusing harmonic radiation at 13 nm

Other than the harmonic photon yield the spatial coherence characteristics and focusability of high-harmonic radiation will be of great importance for a wide range of applications. Therefore, the harmonic sources will have to be characterized and optimized with respect to these properties. The preliminary experiments with diffractive and multilayer focusing optics described in this section represent steps towards this direction.

The Fresnel zone plate described in Sect. 1 has been inserted in the harmonic beam 30 cm downstream of the source. This experiment constitutes, to the best of our knowledge, the first attempt to focus harmonic radiation with an X-ray diffractive optics. In front of the zone plate two 0.2- μm Zr + 0.2- μm Si filters have been placed for blocking the laser light and providing a wavelength band selection. The filters transmit XUV radiation in the spectral band between 12.4 nm and approximately 17 nm (the spectral transmittivity is included in Fig. 6). The harmonic beam diameter at the zone plate is

about 600 μm . The radial intensity distribution of the harmonic beam transmitted through the filters has been recorded with a back-illuminated soft-X-ray CCD camera at a distance of 40 cm from the source.

The results of preliminary experiments aiming at focusing the yield-optimized beam with the Fresnel zone plate at around 13 nm are depicted in Fig. 5. The squares represent the focused diffracted beam as transmitted through a microslit that has been scanned across the XUV beam in the focal plane of the zone plate. The focused diffracted signal has been separated from the one transmitted without diffraction (zeroth order) by detecting the radial intensity distribution with the CCD camera in the far field, where the latter appears as a comparatively narrow intense peak superimposed on a broad pedestal representing the diffracted beam. The scanning position of the slit was inferred from that of the slit projection on the CCD camera produced by the defocused minus first-order diffracted light from the zoneplate, which is simultaneously visible in all camera pictures. Assuming a Gaussian profile of the focused XUV beam and a rectangular spatial transmission function of the slit, deconvolution of data in Fig. 5 yields a focused spot diameter ($1/e^2$ diameter) of ≈ 2 μm . The observed spot size is likely to be limited by chromatic aberration as a consequence of the non-monochromatic illumination of the zone plate. This shortcoming may be avoided in future experiments by selecting a single, harmonic for example by a Mo/Si multilayer mirror (see below). This will pave the way towards focused spot sizes in the sub-micron regime.

Alternatively, the Mo/Si spherical multilayer mirror has been tested as a focusing element for harmonic radiation near 13 nm. Recently, a Mo/Si multilayer was used for focusing laser harmonic radiation emerging from a xenon gas jet near 55 nm and a spot size of ≈ 10 μm could be achieved [23]. Significantly smaller spot sizes of about 0.5 μm have been demonstrated with an X-ray laser at 15.5 nm [24]. The reflectivity of the Mo/Si mirror used in our experiments is shown as a function of wavelength for normal incidence in Fig. 6

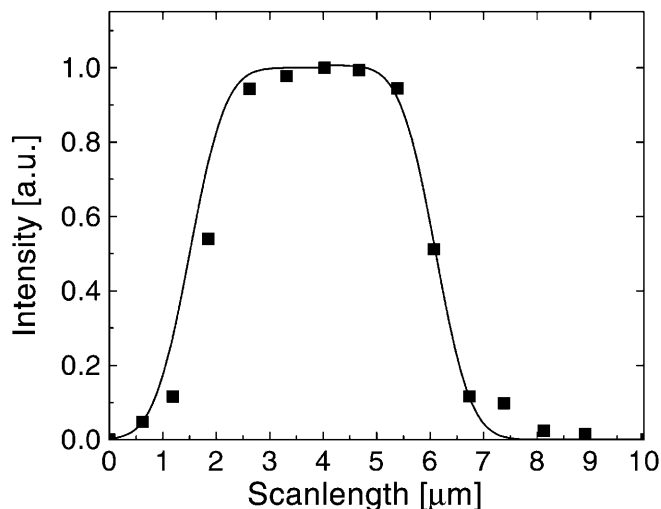


Fig. 5. Intensity of first-order diffracted 13-nm harmonic light focused by a zone plate transmitted through a micro-slit (squares) as a function of slit position. The data have been obtained in a horizontal scan through the focal plane. The fit (line) assumes a Gaussian beam profile and yields a focused beam diameter of $2w_0 = 2.3$ μm

together with the transmittivity of the Zr–Si filter combination. The figure also depicts the harmonic spectrum emerging from the neon target as recorded with a spectrograph made up of a 10000 lines/mm transmission grating and a CCD camera. According to these measurements the mirror reflects most efficiently the 61st harmonic and to some extent the 59th harmonic. It is remarkable that also even harmonics appear in the radiation spectrum of the few-cycle-driven neon target. These unique features, which have not been observed in the spectrum emitted by the same target upon 30-fs illumination, seem to be intimately related to the interaction time confined to just a few cycles and call for further investigations. From a practical point of view, the coalescence of discrete harmonics to a quasi-continuum due to sub-10-fs excitation is quite helpful in maximizing the number of photons directed on a unit area within a unit time, i.e. if maximum peak intensities are required.

The extension of the 13-nm harmonic beam focused with the spherical multilayer mirror has been measured by scanning a knife edge in both orthogonal transverse directions at different positions near the focal region. The mirror was placed 120 cm from the harmonic source where a harmonic beam extension of 2 mm × 2.2 mm was obtained. The beam diameters measured in the horizontal and vertical planes are shown in Fig. 7 as a function of the position along the beam axis. The depicted data have been evaluated from the average of at least three scans at a same position by fitting the signal curves assuming a Gaussian spatial intensity distribution [25]. The full line represents a least-square fit of a propagating Gaussian beam to the data measured in the horizontal plane and yields a spot size (radius) at the beam waist of $w_0 \cong 1.1 \mu\text{m}$ and $M^2 \approx 5$. Measurements in the vertical plane give similar results. The strong astigmatism observed is primarily attributed to a (slight) astigmatism of the fundamental laser beam, which originates from the spherical focusing mirror in front of the target. Optimization of both the laser focusing as well as XUV focusing geometry should allow us to efficiently focus the harmonic photons to within a circular spot of less than 1 μm in diameter.

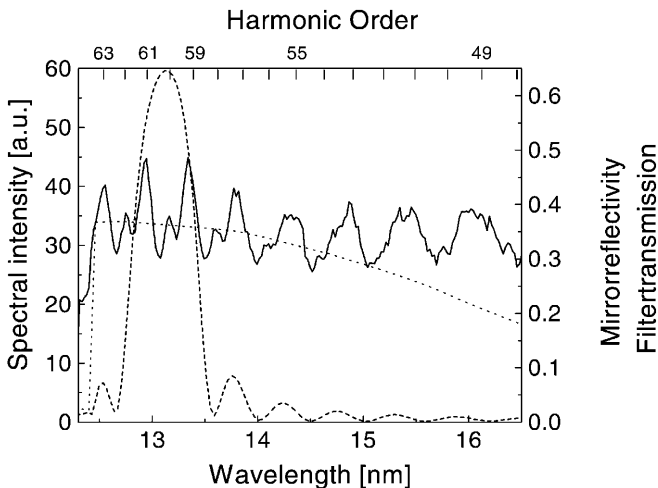


Fig. 6. High-harmonic spectrum (line) from a neon source as transmitted through a 0.2- μm Zr and 0.2- μm Si filter, recorded with a 10000-line/mm transmission grating in comparison with the calculated reflectivity of a 28-layer Mo/Si mirror (dashed) and filter transmission (dotted)

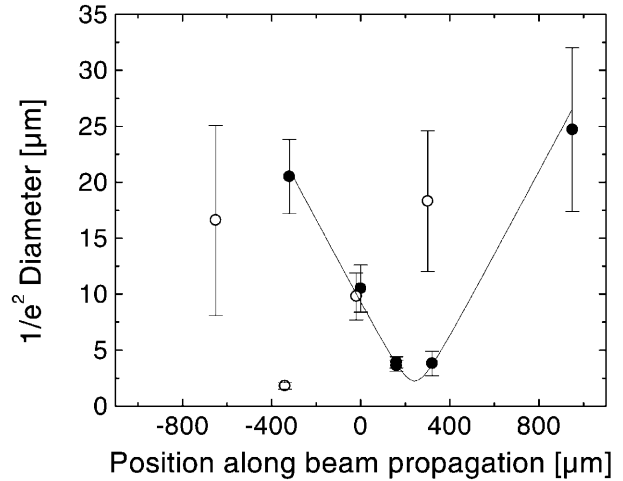


Fig. 7. Gaussian beam diameter of 13-nm harmonic radiation (evaluated from knife-edge measurements described in the text) as a function of position along the beam axis near the focus of a spherical Mo/Si multilayer mirror ($f = 35 \text{ mm}$) in the horizontal (closed circle) and vertical (open circles) plane. Line: fit of a Gaussian beam with $w_0 \approx 1.1 \mu\text{m}$ and $M^2 \approx 5$

5 Conclusion

We have reported absorption-limited high-harmonic generation down to the boundary of the soft-X-ray regime at around 10 nm by using few-cycle sub-10-fs driver laser pulses and demonstrated the focusability of the generated radiation with diffractive and multilayer X-ray optics. Within the 0.7-nm high-reflectivity band of a Mo/Si multilayer mirror centered at 13 nm, the demonstrated few-cycle-driven neon harmonic source emits approximately 10^6 – 10^7 photons/pulse within an estimated pulse duration of $\leq 3 \text{ fs}$. Moderate upgrade of the driver laser and ultimate optimization of focusing holds promise for achieving peak intensities in excess of 10^{13} W/cm^2 at high (kHz) repetition rates for the first time in the soft-X-ray regime. This parameter combination along with the predicted sub-fs duration of spectrally-controlled few-cycle-driven harmonic pulses may open up the way to nonlinear X-ray spectroscopy and allow us to trace inner-shell electron relaxations dynamics.

Acknowledgements. This work has been sponsored by the Austrian Science Fund, grants Y44-PHY and P12631-PHY, the Austrian Ministry of Science and Transportation, and by the state NRW in Germany (Bennigsen-Foerdner research award). We thank U. Kleineberg and E. Majkova for advice concerning multilayer technology.

References

1. A. L'Huillier, P. Balcou: *Phys. Rev. Lett.* **70**, 774 (1993)
2. J.J. Macklin, J.D. Kmetec, C.L. Gordon III: *Phys. Rev. Lett.* **70**, 766 (1993)
3. Z. Chang, A. Rundquist, H. Wang, M.M. Murnane, H.C. Kapteyn: *Phys. Rev. Lett.* **79**, 2967 (1997)
4. C. Spielmann, N.H. Burnett, S. Sartania, R. Koppitsch, M. Schnürer, C. Kan, M. Lenzner, P. Wobruschek, F. Krausz: *Science* **278**, 661 (1997)
5. S. Sartania, Z. Cheng, M. Lenzner, G. Tempea, C. Spielmann, F. Krausz: *Opt. Lett.* **22**, 1562 (1997)
6. G. Schmahl, D. Rudolph, G. Schneider, J. Thieme, T. Schliebe, B. Kaulich, M. Hettwer: *Microelectron. Eng.* **32**, 351 (1996)
7. U. Kleineberg, H. J. Stock, D. Menke, O. Wehmeyer, U. Heinzmann: *Proc. SPIE* **3150**, 18 (1997)

8. M. Jergel, V. Holy, E. Majkova, S. Luby, R. Senderak, H.J. Stock, D. Menke, U. Kleineberg, U. Heinzmann: *Physica B* **253**, 18 (1998)
9. M. Schnürer, C. Spielmann, P. Wobrauschek, C. Strelt, N.H. Burnett, C. Kan, K. Ferencz, R. Koppitsch, Z. Cheng, T. Brabec, F. Krausz: *Phys. Rev. Lett.* **80**, 3263 (1998)
10. M. Schnürer, Z. Cheng, M. Hentschel, G. Tempea, P. Kálman, T. Brabec, F. Krausz: *Phys. Rev. Lett.* **83**, 722 (1999)
11. A. Dalgarno, A.E. Kingston: *Proc. Roy. Soc.* **A259**, 424 (1966)
12. http://www-cxro.lbl.gov/optical_constants/
13. A. Rundquist, C.G. Durfee III, Z. Chang, C. Herne, S. Backus, M.M. Murnane, H.C. Kapteyn: *Science* **280**, 1412 (1998)
14. M. Lewenstein, P. Balcou, M.Yu. Ivanov, A. L'Huillier, P.B. Corkum: *Phys. Rev. A* **49**, 2117 (1994)
15. M.V. Ammosov, N.B. Delone, V.P. Krainov: *Sov. Phys. JETP* **64**, 1191 (1986)
16. E. Constant, D. Garzella, P. Breger, E. Mével, C. Dorrer, C. Le Blanc, F. Salin, P. Agostini: *Phys. Rev. Lett.* **82**, 1668 (1999)
17. P. Salières, A. L'Huillier, M. Lewenstein: *Phys. Rev. Lett.* **74**, 3776 (1995)
18. A. Scrinzi, M. Geissler, T. Brabec: *Phys. Rev. Lett.* **83**, 706 (1999)
19. G. Tempea, M. Geissler, M. Schnürer, T. Brabec: to be published in *Phys. Rev. Lett.* **84**, no 19 (2000)
20. T. Ditmire, J.K. Crane, H. Nguyen, L.B. DaSilva, M.D. Perry: *Phys. Rev. A* **51**, R902 (1995)
21. G. Sommerer, H. Rottke, W. Sandner: *Laser Phys.* **9**, 430 (1999)
22. Recently Y. Tamaki et al. (Y. Tamaki, J. Itatani, Y. Nagata, M. Obara, K. Midorikawa: *Phys. Rev. Lett.* **82**, 1422 (1999)) reported improved conversion efficiencies down to 15 nm, which were attributed to self guiding of 100-fs driver pulses in neon. The maximum coherent signal emission has been obtained from a target characterized by a product of interaction length and gas density that is by a factor of 4–5 lower as compared to that yielding maximum coherent emission in our work. Yet, the authors claim a conversion efficiency of 10^{-6} , in obvious contradiction with our results
23. L. Le Déroff, P. Salières, B. Carré: *Opt. Lett.* **23**, 1544 (1998)
24. T. Ohchi, N. Yamaguchi, C. Fujikawa, T. Hara: *J. Electron. Spectrosc. Relat. Phenom.* **103** (Special Issue SI), 943 (1999)
25. A.E. Siegmann: *SPIE* **1224**, 2 (1990)